Nuclear Materials and Energy 12 (2017) 433–440

Contents lists available at ScienceDirect

Nuclear Materials and Energy

journal homepage: www.elsevier.com/locate/nme

Beryllium layer response to ITER-like ELM plasma pulses in QSPA-Be

N.S. Klimov[a,g,*], V.L. Podkovyrov[a], I.B. Kupriyanov[b], J. Linke[c], R.A. Pitts[d], V.M. Safronov[e], D.V. Kovalenko[a], Th. Loewenhoff[c], C.P. Lungu[f], G. Pintsuk[c], G. De Temmerman[d], A.D. Muzichenko[a], A.A. Markin[b], P.N. Taratorkin[b], N.E. Zabirova[b], A.M. Zhitlukhin[a]

[a] SRC RF TRINITI, ul. Pushkovykh, vladenie 12, Troitsk, Moscow 108840, Russia
[b] Bochvar Institute, ul. Rogova, 5a, Moscow 123098, Russia
[c] Forschungszentrum Jülich GmbH, Jülich D-52425, Germany
[d] ITER Organization, Route de Vinon-sur-Verdon, CS 90 046, St. Paul Lez Durance Cedex, 13067, France
[e] Institution Project center ITER, Akademika Kurchatova pl., 1, Moscow 123182, Russia
[f] National Institute for Laser, Plasma and Radiation Physics, Bucharest 077125, Romania
[g] National Research Nuclear University «MEPhI», Kashirskoe sh. 31, Moscow 115409, Russia

ARTICLE INFO

Article history:
Received 15 July 2016
Revised 16 December 2016
Accepted 10 January 2017
Available online 21 March 2017

Keywords:
ITER
High heat flux
Thermal shock
Beryllium
Tungsten
Coating

ABSTRACT

Material migration in ITER is expected to move beryllium (Be) eroded from the first wall primarily to the tungsten (W) divertor region and to magnetically shadowed areas of the wall itself. This paper is concerned with experimental study of Be layer response to ELM-like plasma pulses using the new QSPA-Be plasma gun (SRC RF TRINITI). The Be layers (1 → 50 μm thick) are deposited on special castellated Be and W targets supplied by the ITER Organization using the Thermionic Vacuum Arc technique. Transient deuterium plasma pulses with duration ~0.5 ms were selected to provide absorbed energy densities on the plasma stream axis for a 30° target inclination of 0.2 and 0.5 MJm^{-2}, the first well below and the second near the Be melting point. This latter value is close to the prescribed maximum energy density for controlled ELMs on ITER. At 0.2 MJm^{-2} on W, all Be layer thicknesses tested retain their integrity up to the maximum pulse number, except at local defects (flakes, holes and cracks) and on tile edges. At 0.5 MJm^{-2} on W, Be layer melting and melt layer agglomeration are the main damage processes, they happen immediately in the first plasma impact. Melt layer movement was observed only near plasma facing edges. No significant melt splashing is observed in spite of high plasma pressure (higher than expected in ITER). Be layer of 10 μm thick on Be target has higher resistance to plasma irradiation than 1 and 55 μm, and retain their integrity up to the maximum pulse number at 0.2 MJm^{-2}. For 1 μm and 55 μm thick on Be target significant Be layer losses were observed at 0.2 MJm^{-2}.

1. Introduction

The wall panels of the ITER main chamber will be almost completely armored with beryllium (Be) [1,2]. It is expected that Be eroded from the first wall will migrate to the W divertor plates and deposit there to form layers [3]. This layer may protect the W from a direct plasma action and can decrease the flow of W to the core plasma, but is also expected to be the main source of fuel retention in ITER and can lead to the formation of significant dust sources if the layers disintegrate, for example under transient energy pulses. The redeposited Be layers are expected on the magnetically shadowed areas of the Be first wall (FW) panels also. The experimental data on Be behavior under the expected transient loads are insufficient for assessments of the PFC lifetime and acceptable transient heat loads. Experiments with Be are complicated because of toxicity of Be dust and they require special operating conditions.

To investigate Be erosion under the ITER-like plasma and photonic heat loads, a new QSPA-Be facility was designed in the SRC RF TRINITI and assembled in the Be cell of the Bochvar Institute. This facility is a modernized variant of the QSPA-T plasma gun which was used for the divertor PFC testing under ITER-like transient heat loads [4–8]. Both facilities provide hydrogen (or deuterium) plasma heat loads related to ITER ELMs or disruptions in the range of 0.2–5 MJm^{-2} (pulse duration ~0.5 ms) and photon radiation heat loads relevant to ITER mitigated disruptions up to 1 MJm^{-2} (pulse duration ~0.5 ms) [9]. The first results of Be PFC

* Corresponding author at: Troitsk, ul. Pushkovikh, vladenie 12, SRC RF TRINITI, Moscow 108840, Russian Federation.
E-mail address: klimov@triniti.ru (N.S. Klimov).

http://dx.doi.org/10.1016/j.nme.2017.01.012

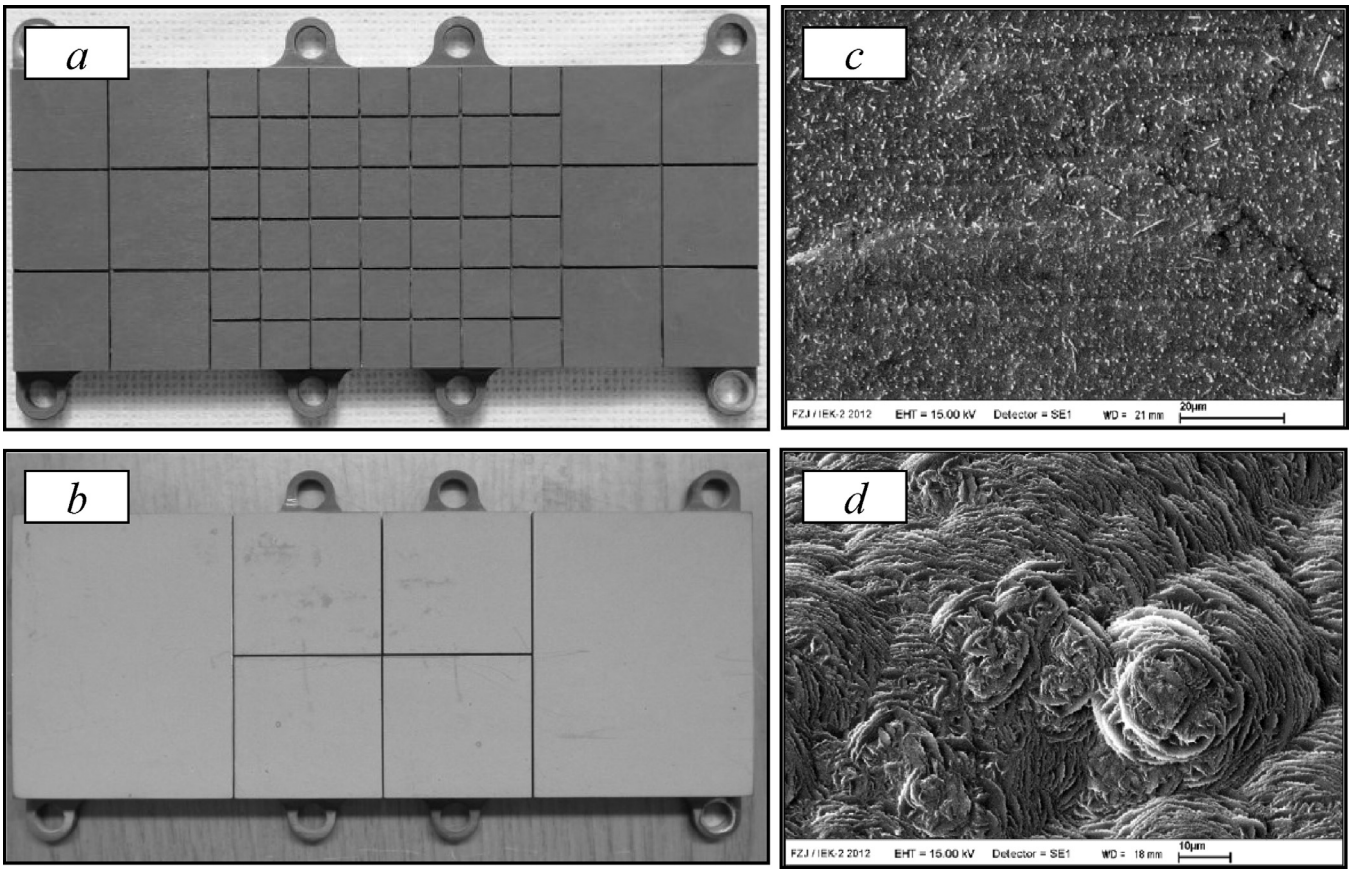

Fig. 1. Top view of the targets ((a) – W divertor PFCs, (b) – Be FW PFCs) and typical SEM images of the Be coatings ((c) – 1 µm, (d) – 55 µm).

erosion under ELM-like plasma heat loads obtained with QSPA-Be are already published [10–12]. These experiments used Be plates and mock-up of the beryllium ITER first wall PFCs from Russian Be grade TGP-56FW and US Be grade S65-C, which are the candidates for the ITER first wall (FW). The targets were exposed to the plasma heat loads of 0.2 – 1.0 MJm^{-2}, at initial base temperatures in the range 250 – 500 °C and with pulse duration of 0.5 ms.

The present work concerns the next step of these investigations which includes plasma testing of mock-ups of the ITER tungsten divertor target and mock-ups of ITER FW Be panel. The W divertor targets and Be FW panels were preliminary coated with thin Be layers of 1, 10, and 55 µm thickness. Originally manufactured in the EU, under the previous European Fusion Development Agreement, the targets were transferred to Fusion For Energy and finally to IO ownership. The Be coatings were applied in Romania at the National Institute for Laser, Plasma and Radiation Physics in Bucharest.

2. Experimental techniques and conditions of the targets exposure

The targets were specially provided for these experiments by IO. Each tungsten target (Fig. 1a) consist of 3 mm tungsten layer, which were brazed (by 2 mm copper layer) on the supporting stainless steel plate of 60 × 150 mm^2. The tungsten surface were castellated to 42 tungsten elements of 9.5 × 9.5 mm^2 surface area and 12 tungsten elements of 19.5 × 19.5 mm^2 surface area. The gaps between neighbor elements with 0.5 mm.

The tungsten surface of the targets was coated with thin Be layers in Romania using the Thermionic Vacuum Arc technique under the following conditions. Pressure in the vacuum chamber was in the range (4.5 – 7.5)·10^{-7} torr during deposition. Base substrate temperature was 400 °C. Deposition rate was in the range of 2–5 nm/s. This technique was used for ITER-like wall project at JET [13,14]. Different thickness of Be coating were provided by varying of deposition time. Three targets were provided with Be layer thickness of 1, 10, and 55 µm for the experiments. The one target without Be layer was also used in the experiment for comparison.

The SEM views of deposited Be layer depended on layer thickness and were practically independent of substrate (Be or W). Typical SEM images are presented on the Fig. 1c and d. The Be layers of 10 and 55 µm were faced by rosebud structures with diameter of several micrometers. For 1 µm layer the significantly fine-grained structure was observed. But for all thicknesses the continuous (compact) layer without through pores were performed.

Each Be target (Fig. 1b) consist of 8.5 mm beryllium (S65C) layer, which were brazed (by 2 mm copper layer) on the supporting stainless steel plate of 60 × 150 mm^2. The beryllium surface were castellated to 4 elements of 29.5 × 29.5 mm^2 surface area and 2 elements of 59.5 × 44.5 mm^2 surface area. The gaps between neighbor elements with 0.5 mm. The beryllium surface of the targets was also coated with thin Be layer. Three targets were used with Be layer thickness of 1, 10, and 55 µm.

The general schemes of target plasma exposure at the QSPA-Be facility are presented in Fig. 2a. The exposed target with infrared heater is placed under direct plasma action at the distance of 60 cm from the plasma gun. The incidence angle of the plasma flow can be varied from 0 up to 80° (60° in present experiments). The results of some previous experiments performed using this loading scheme are described in the [4–8,10–12].

The infrared heater which provides the target preheating before the plasma exposure and maintains the target surface temperature before each plasma pulse at a fixed level in the range 20 – 500 °C. In all cases of present work, the target heater was used to set a

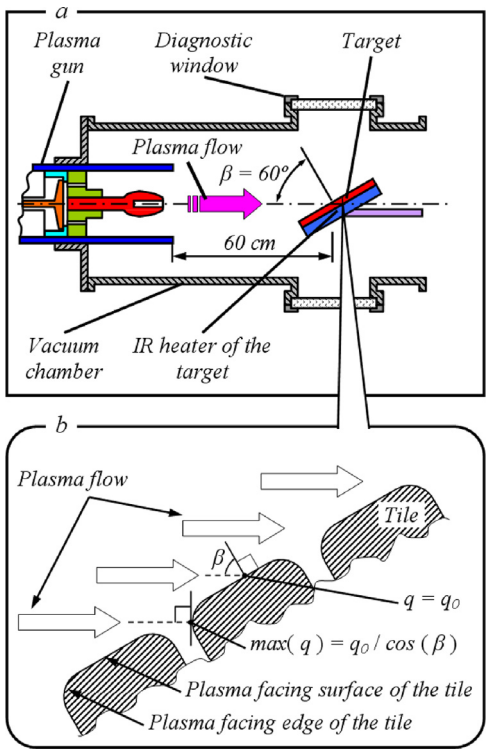

Fig. 2. The scheme of plasma exposure of the target: (a) — target placing into vacuum chamber of the QSPA-Be; (b) — geometry of plasma action.

base temperature of 250 °C, chosen to approximately represent regions of the ITER W divertor plate away from the strike points in regions where Be layers are expected to grow more readily due to migration from the main chamber. The target surface was oriented at incidence angle of 60°, giving an angle of 30° between the plasma beam axis and the target surface. This angle is required to maintain sufficient power flux density on the target surface to be relevant to a subset of expected ELM energy densities on ITER, but does not, of course, match the grazing incidence angles that will occur at the ITER divertor targets. Simple geometric analysis (Fig. 2b) indicates that due to the inclined plasma action, the maximum energy density on the plasma facing edges of the tiles exceeds by a factor of two that falling on the tile top surface.

The Mo shield was used in the experiment (Fig. 3a). Mo shield restricts the exposed area of the target and allows only half of the target surface to be exposed, increasing the number of experiments possible.

The power supply system of the QSPA-Be facility provides different waveforms of the discharge power. For present experiment the trapezoidal pulse waveform was applied. This pulse shape includes short rise phase of 0.05 ms duration, a roughly constant flat-top phase of duration 0.5 ms followed by an exponential decrease of 0.4 ms (from 100% to 10% of the peak value).

For the chosen heat loads the results of the early experiments with bulk Be targets without coating [12] were used. According to those experiments for energy densities below ~0.5 MJm^{-2} no melting of the Be layer is expected, if base temperature do not exceed 250 °C. These experimental results are agreed with numerical calculation performed in present work by means of the code RACLETTE [15–16]. These calculations were based on the experimentally measured pulse waveforms and assume ideal thermal contact of the Be coating layer with the W surface. So for 0.2 MJm^{-2} on the top surface, a maximum value of ~0.4 MJm^{-2} should be incident on the plasma facing edges, still below the Be layer melt threshold (~0.5 MJm^{-2}).

The regimes of QSPA-Be facility were selected to provide absorbed energy density values of 0.2 (first stage) below melting point and 0.5 MJm^{-2} (second stage) near the melting point on the plasma stream axis. For this two peak values the local value of the absorbed energy density varies across the target surface in the range 0.04 – 0.2 MJm^{-2} and 0.1 – 0.5 MJm^{-2} respectively. The local energy density was obtained by using special calorimeters with spatial resolution. There were two calorimeters used from tungsten and niobium. Both refractory metals do not melted and evaporated under mentioned heat loads, so the calorimeters fully absorbed plasma energy which are come to calorimeter surface. These calorimeters are an usual diagnostics of QSPA-Be facility, which were described early [4–8,10–12]. The 2-D load distribution on target surface can be approximated by a Gaussian function with half-width of 12 cm in the longitudinal direction and 6 cm in the transversal direction (Fig. 3b). The deuterium plasma was used in the experiments. The direct pressure of the plasma flow at the normal plasma action on the plasma flow axis equals 1.0 bar (first stage) and 2.5 bar (second stage). Due to inclined plasma action ($\beta = 60°$) the pressure on the target surface is lower in a factor of 2 approximately than measured value at the normal plasma action. Nevertheless plasma pressure exerted by the QSPA pulse exceeds one expected in ITER for ELM pulses. The discrepancy is of order a factor 10. This fact was taken into account under analyzing of obtained experimental data.

During the first stage of the experiments each of the three Be coated (1, 10 and 55 μm thickness) targets were exposed to 50 pulses at 0.2 MJ/m^2. The Mo mask was used to protect one half of the targets, allowing exposures on fresh surfaces to be made in the second stage. During the latter (second stage), the unexposed halves of the two targets (with Be coating of 10 and 50 μm thickness) were exposed to 2 pulses at increased energy density of 0.5 MJ/m^2 (~1.0 MJ/m^2 on the tile edges).

The exposed targets were photographed, scanned by optical scanner with high special resolution and their surfaces observed by means of an optical microscope. Typical images of the exposed target are presented in the Fig. 3a, c and d. The observation was performed after different number of pulses (after 2, 10 and 50 pulses). The exposed targets were investigated by means of scanning electron microscopy (SEM) and energy-dispersive X-ray spectroscopy (EDX).

3. Experimental results and discussion

3.1. Be layer behavior on W target under plasma exposure

According to optical observation the following main damage processes were identified for Be layers on the W surface at heat loads of 0.2 MJm^{-2}: (a) the artifacts of the melting of the-plasma facing edges of the tiles; (b) changing of the color of the exposed surface (Fig. 3c); (c) spots on the exposed surface (Fig. 4a and d) with sizes from 10 μm up to several millimeters;. No damage was observed on the pure W surface (uncoated target) without Be layer (no surface coloring, spots, holes, cracks, and edges melting), which were exposed at the same conditions (Fig. 3a). These results show that the observed damage on the coated targets must be largely a consequence of the Be layer.

The smoothing and brightening of the plasma-facing edges of the tiles are the result of Be melting on the edges. This point is confirmed by the SEM analysis. Melting Be layer on the plasma facing edges is a result of inclined plasma action to macrobrush surface of the target. According presented above geometrical analysis (Fig. 2b) the area with energy density higher than on the top tile surface is existed on the plasma facing edge.

Analysis of the color transformation (bluish and grey-brown areas) indicates that this is a result of Be deposition. The different

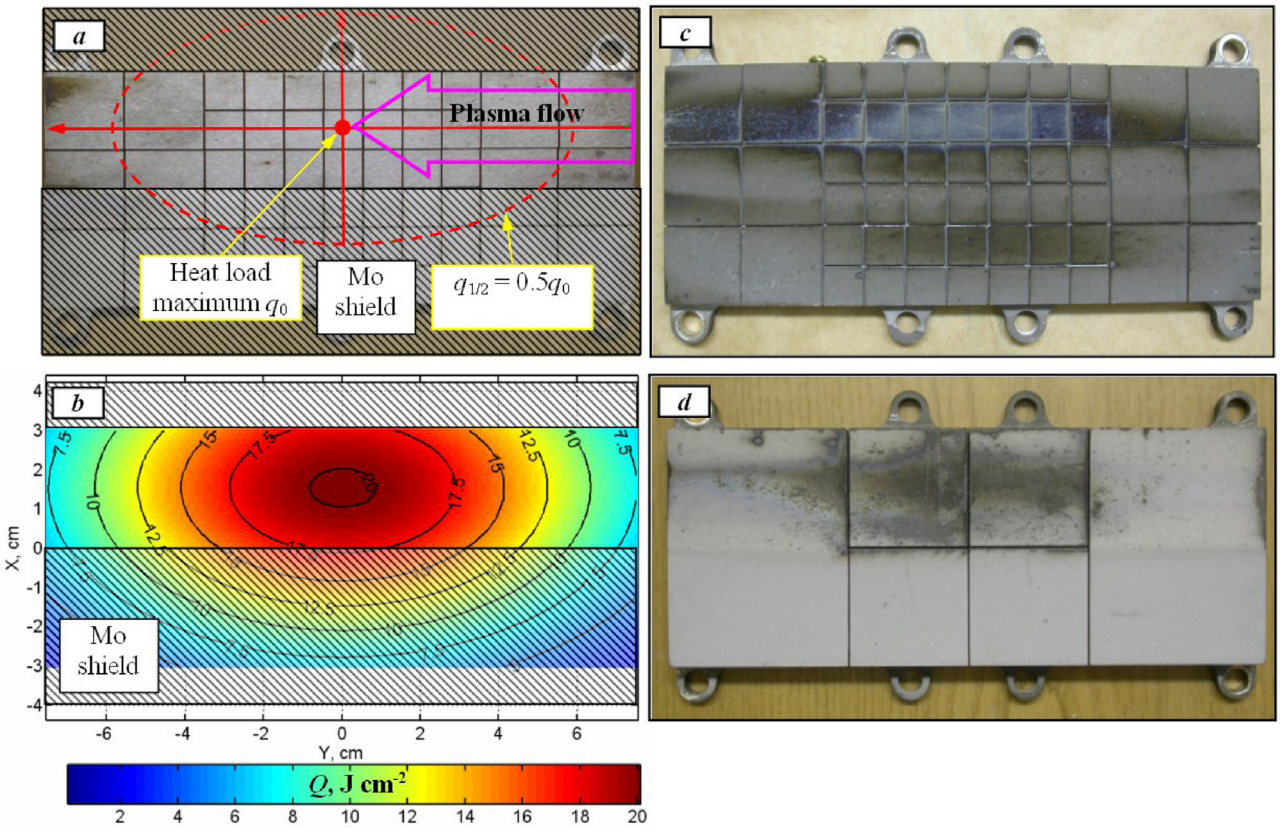

Fig. 3.. Energy density distribution on the target surface (a, b), the scheme of the Mo shield placement (a, b) and typical top view of exposed targets (a, c, d): (a) — uncoated W target ($q_0 = 0.2$ MJm^{-2}, $N = 10$ pulses); (b) — heat load distribution on the target surface ($q_0 = 0.2$ MJm^{-2}); (c) — W target with 55 μm Be layer ($q_0 = 0.2$ MJm^{-2}, $N = 10$ pulses); (d) — Be target with 55 μm Be layer ($q_0 = 0.2$ MJm^{-2}, $N = 50$ pulses).

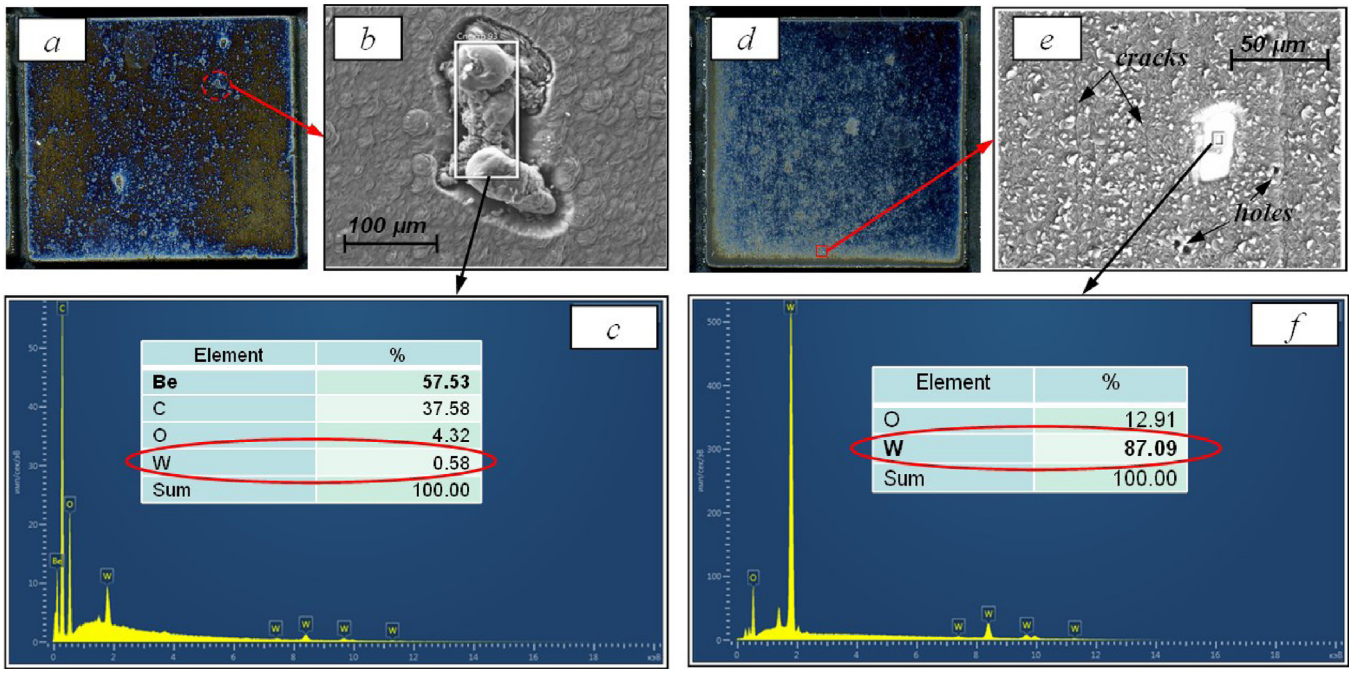

Fig. 4. Typical optical images (a, d), SEM images (b, e), and EDX spectrograms (c, f) of W target with Be layer after plasma exposure: (a), (b), (c) — W target with 55 μm Be layer ($q_0 = 0.2$ MJm^{-2}, $N = 10$ pulses); (d), (e), (f) — W target with 10 μm Be layer ($q_0 = 0.2$ MJm^{-2}, $N = 10$ pulses).

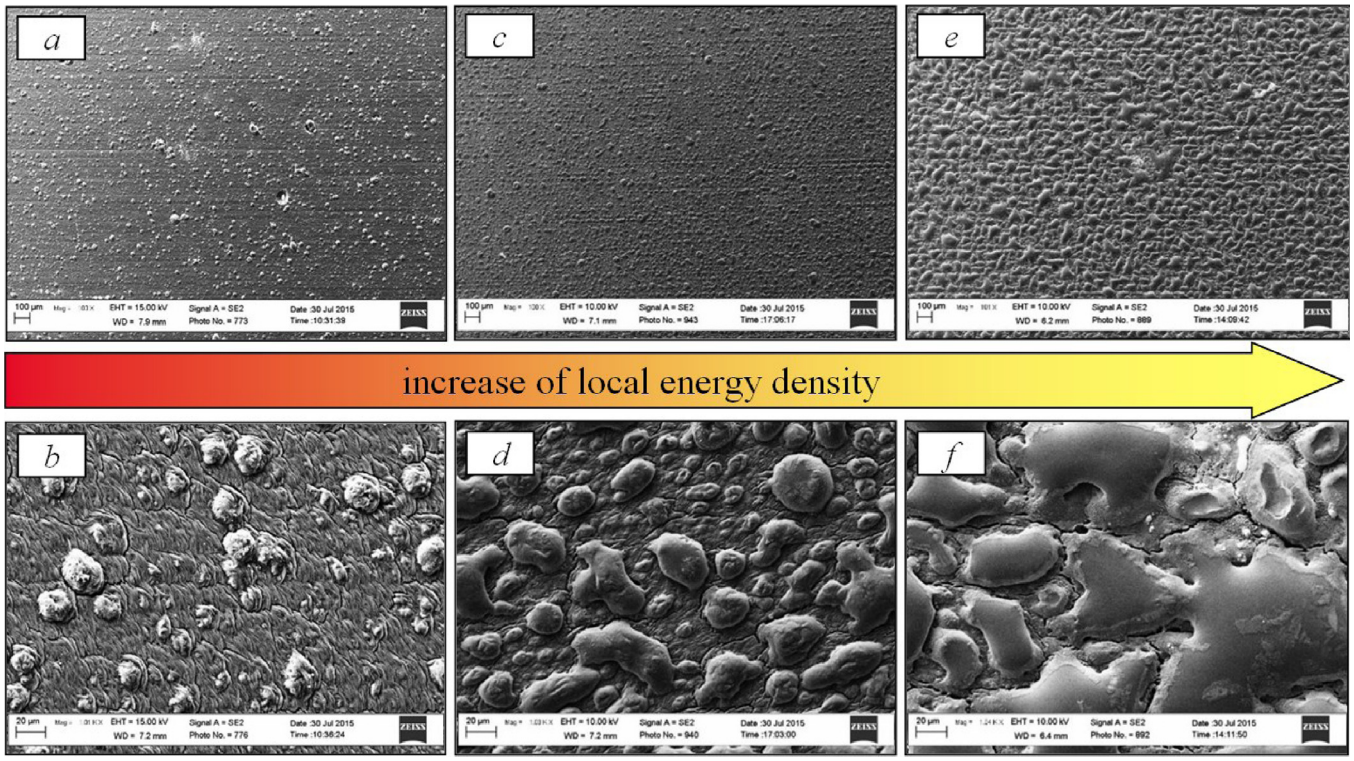

Fig. 5. Morphology of the exposed Be layer surface on W target as a function of the local energy density (W target with 55 μm Be layer, $q_0 = 0.5$ MJm^{-2}, $N = 2$ pulses): (a), (b) – $q = 0.2$ MJm^{-2}; (c), (d) $q = 0.4$ MJm^{-2}; (e), (f) – $q = 0.5$ MJm^{-2}.

areas of the Be surface have different temperatures during plasma exposure. Significant differences occur in the evaporation rate between the base target surface and the edges. The Be evaporated from higher temperature regions (edges or defects) can deposit onto colder regions. As a result, a thin layer (several tens of nanometers) forms on the target surface and leads to color transformation [17]. Evaporation and sputtering of tungsten are significantly lower than that for Be so that color transformation on the uncoated W target was not observed.

Observed local rate of Be evaporation significantly exceeds the level, which we calculated for case of perfect thermal conductivity and undeveloped Be surface. This evaporation may lead to vapor shielding effects, which are not expected in the investigated heat load range according calculation.

The combination of the SEM and EDX analysis permits some clarification as to the nature of the spots observed on the surface, and a rough classification of the type of defects. Typical optical images, SEM images, and corresponding X-ray spectrograms illustrating this classification are presented in Fig. 4. According to the SEM/EDX analysis the spots observed in the optical images mainly correspond to two types of defects of the Be layer. The first type are agglomerations of the Be in the form of flakes or droplets (Fig. 4a–c). SEM observation indicates that significant number of such agglomerations are existed before exposure. The plasma exposure lead to damages of the prominences areas mainly. The melting of the microstructure of prominences areas, which will be discussed below (Fig. 5), entails the reflectivity increase of these areas.

Defects of the second type (Fig. 4d–f) are areas of Be layer delamination. The significant fraction of such areas seems to be associated with Be layer defects existing before plasma exposure. Local Be layer delamination during plasma action cannot, however, be excluded. Optical observations indicate that significant number of light spots arises already after first 10 pulses and additional pulses do not lead to the considerable further increase of defects number.

According to SEM observations at higher magnifications, with the exception of edges and local macroscopic defects existing before exposure, the Be layer retains a continuous structure which is closed to the one observed before exposure for pulse energy densities of 0.2 MJ/m^2 (which is less than the Be melt threshold). The Be layer contains only defects (Fig. 4e) in the form of microscopic holes with diameters of 1 – 5 μm, and microcracks with crack width ~0.4–1.5 μm. This Be layer behavior depend on only local value of the energy density. This point is confirmed by comparison data from the central part of the target of the first stage ($q_0 = 0.2$ MJm^{-2}) and the peripheral target areas with the same local energy density of the second stage ($q_0 = 0.5$ MJm^{-2}).

The impact of the surface melting to Be layer damage is increase with energy density (Fig. 5). At the heat loads of 0.2 MJm^{-2} after 2 pulses (Fig. 5a and b) the SEM view of the exposed surface practically identical to one before exposure (Fig. 1d) besides slightly damages of the prominences rosebud structure. But at the heat loads of 0.4 MJm^{-2} the significant melting of the prominences on the top tile surface was observed (Fig. 5b and d) already after 2 pulses. At the heat loads of 0.5 MJm^{-2} the melting of the full Be layer surface was appearing (Fig. 5e and f) not only on the edges but also on the top surface. Optical observation indicates that Be layer melting and agglomeration of the melt material are the main damage processes on the targets exposed to the pulsed heat loads of 0.5 MJm^{-2} (see Fig. 5). Melt layer movement, which is observed mainly near plasma facing edges, lead to fully elimination Be layer near plasma facing edges even for maximum thickness of Be layer (55 μm) already after 2 pulses. But no significant melt splashing is observed, despite the far higher plasma pressure than expected in ITER.

3.2. Be layer behavior on Be target under plasma exposure

Typical photos of the exposed targets after the first stage of the exposure are presented in Fig. 3d. According to visual obser-

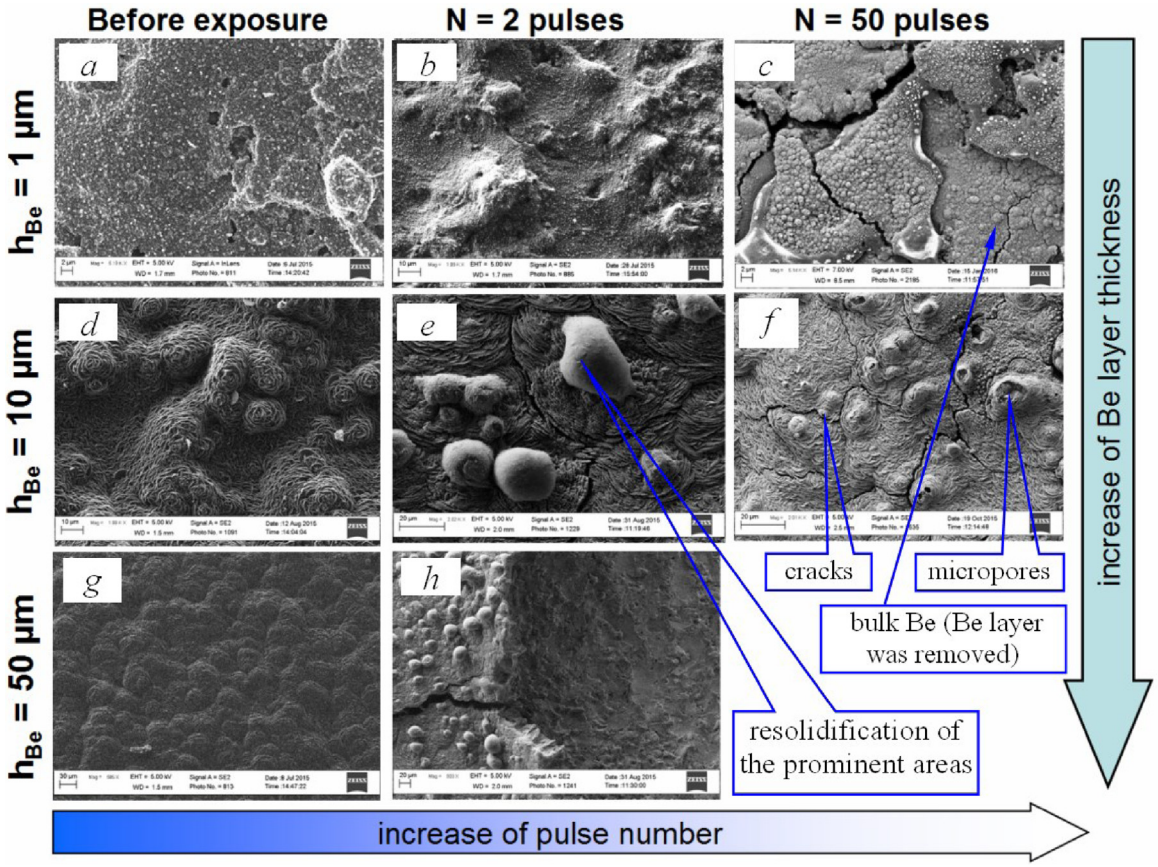

Fig. 6. Morphology of the exposed Be layer surface on Be target as a function of pulse number and layer thickness at the heat load of $q_0 = 0.2\ \mathrm{MJm^{-2}}$: (a), (b), (c) — 1 μm Be layer; (d), (e), (f) — 10 μm Be layer; (g), (h) — 55 μm Be layer; (a), (d), (g) — before exposure; (b), (e), (h) — after $N = 2$ pulses; (c), (f) — after $N = 50$ pulses.

vation the following main damage processes were identified at the heat loads of $0.2\ \mathrm{MJm^{-2}}$: (a) changing of the color of the exposed surface; (b) the spots on the exposed surface; (c) the artifacts of the melting of the-plasma facing edges of the tiles; (d) the macroscopic damage of the Be layer due to flaking (only for the layer of 1 μm and 55 μm thickness).

Analysis of the color transformation in the peripheral areas indicates that this is a result of Be deposition. This process was observed in the experiments with W and described above as well as the artifacts of the melting of the plasma facing edges of the tiles (edges melting, edges smoothing and jets formations), which are the result of inclined plasma action (see Fig. 2b). Optical and SEM observations indicate that the plasma facing edges erosion of Be targets covered by Be layer is more intense as compare to W targets covered by Be layer of the same thickness and exposed at the same conditions. This point is explained by maximum possible value of the melt layer thickness. In the case of W targets covered by Be layer the melt layer thickness can not be higher than the Be layer thickness because melting threshold of W did not exceeds. In the case of Be targets covered by Be layer the melt layer thickness may be higher due to melting of bulk (substrate) Be. The melt layer mobility increases with melt layer thickness due to decreasing of the Rayleigh friction force.

The spots on the exposed surface of the target with 1 μm Be layer are the result of two processes (Figs. 6a–c and 7a): (1) local delamination of the Be layer; (2) local melting of the Be layer. As a result of analysis of the SEM images the following main damage processes of 1 μm Be layer were identified: cracks formation on the beryllium layer; elimination of the some area of the Be layer due to flaking (the maximum size of the peels is 10 – 50 μm); changing of the Be layer microstructure due to melting and resolidification of the Be layer surface. The flaking of 1 μm Be layer after 50 plasma pulses lead to significant Be layer losses in the range of 10 – 40%, which value is depend on location on the exposed surface.

The spots on the exposed surface of the target with 10 μm Be layer (Fig. 7b) are mainly the result of local melting (Fig. 6d–f). The comparative analysis is illustrated on the Fig. 6 display different behavior for 1 μm and 10 μm Be layers. So cracks formation was also observed on the targets with Be layer thickness of 1 μm and 10 μm. But in the case of 10 μm Be layer this process was not lead to flaking. Elimination of the 10 μm Be layer after 50 plasma pulses of $0.2\ \mathrm{MJm^{-2}}$ was not observed. For 10 μm Be layer changing of the Be layer microstructure due to melting and resolidification was observed mainly on the prominent areas of the Be layer surface. Some number of resolidified area contain micropores which may be the result of gas outlet. The 10 μm Be layer retains its integrity after 50 plasma exposure at energy density of $0.2\ \mathrm{MJm^{-2}}$.

The macroscopic damage of the Be layer due to macroscopic flaking (the maximum size of the peels is 1 – 5 mm) of significant area of the layer was observed only on the target with 55 μm Be layer thickness. The catastrophic damages were observed already after two pulses (Figs. 6h and 7c). After this the plasma exposure of the target at the energy density of $0.2\ \mathrm{MJm^{-2}}$ was stopped. Such behavior indicates to lower adhesion of 55 μm Be layer as compare with thinner cases (Fig. 7).

The lower adhesive and thermal contact of 55 μm Be layer as compare with thinner cases lead to significantly different behavior at the higher heat loads of $0.5\ \mathrm{MJm^{-2}}$. Typical photos of the exposed targets after the second stage of the exposure are presented in Fig. 7e and f. For Be target with 10 μm Be layer the following

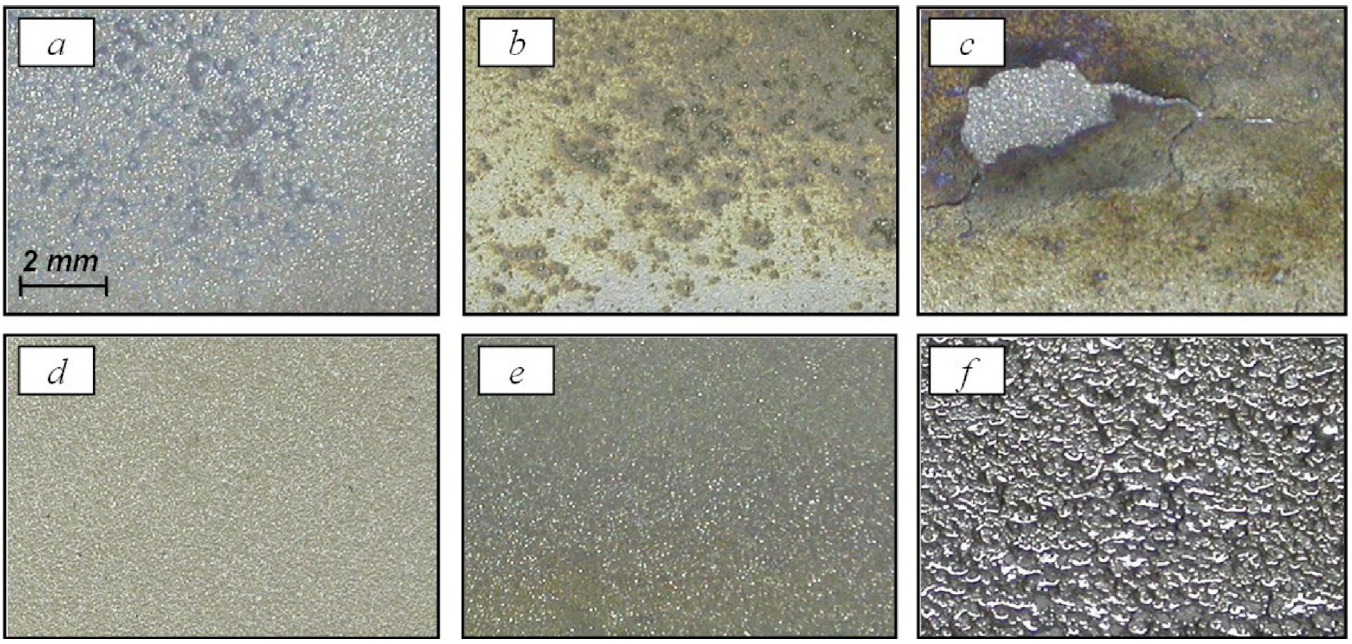

Fig. 7. Optical images of the exposed Be layer surface on Be target as a function of heat load and layer thickness: (a) — 1 μm Be layer, $q_0 = 0.2\ MJm^{-2}$, $N = 50$ pulses; (b) — 10 μm Be layer, $q_0 = 0.2\ MJm^{-2}$, $N = 50$ pulses; (c) — 55 μm Be layer, $q_0 = 0.2\ MJm^{-2}$, $N = 2$ pulses (d) — 10 μm Be layer before exposure; (e) — 10 μm Be layer, $q_0 = 0.5\ MJm^{-2}$, $N = 2$ pulses; (f) — 55 μm Be layer, $q_0 = 0.5\ MJm^{-2}$, $N = 2$ pulses.

processes were observed at the heat loads of $0.5\ MJm^{-2}$: higher edges damage (smoothing and splashing) as compare with lower heat load ($0.2\ MJm^{-2}$); higher local melting of the exposed surface as compare with lower heat load ($0.2\ MJm^{-2}$).

The behavior of the 55 μm Be layer at the heat load of $0.5\ MJm^{-2}$ was significantly differ from $0.2\ MJm^{-2}$ and from the 10 μm Be layer. The significant area of the Be layer (practically full area of the small tiles in the target center and partially the area of the big tiles — total more than 50% of the plasma exposed surface) was fully remelted and resolidified after two plasma pulses at $0.5\ MJm^{-2}$. As a result of such resolidification significant part of the Be layer material may be soldered with bulk beryllium. The optical observations also indicate that Be layer was eliminated from significant macroscopic regions on the central part of the target surface. This may be as the result of flaking during first plasma pulse. Additional investigations are needed for confirmation of the last two points.

The target with 10 μm Be layer display also perfect performance at the higher heat load of $0.5\ MJm^{-2}$ (Fig. 7e) as compare with 55 μm Be layer (Fig. 7f). The SEM images of the 10 μm Be layer after 2 pulses at $0.5\ MJm^{-2}$ are very like to SEM images of the 10 μm Be layer after 50 pulses at $0.2\ MJm^{-2}$. The main observed damage processes: cracks formation; melting and resolidification of the prominent area of the Be layer surface; the micropores, which may be the result of gas outlet. The 10 μm Be layer retains its integrity after 2 plasma exposure at energy density of $0.5\ MJm^{-2}$. In the case of 55 μm Be layer after 2 plasma pulses at $0.5\ MJm^{-2}$ (Fig. 7f) the full surface of Be layer on the central tiles was remelted (resolidified) and significant area of bulk Be was observed.

Optical observation indicates and SEM analysis (presented below) confirms the point that the 10 μm Be layer retains its integrity after 50 plasma exposure at energy density of $0.2\ MJm^{-2}$ and after 2 at $0.5\ MJm^{-2}$ except plasma facing edges. The 10 μm Be layer on the bulk Be surface display lower erosion rate as compare with 1 μm and 55 μm Be layer. This result indicates to existence of optimal thickness of Be layer on the bulk Be surface, which is correspond to minimal erosion rate and maximum lifetime.

4. Conclusion

The formation of local macroscopic defects (holes and flakes with sizes from 10 μm up to several millimeters) and local microscopic defects (micropores with diameters of 1–5 μm, microcracks with crack width ~0.4–1.5 μm), tile edges melting, and material evaporation, which lead to material redeposition and surface coloring, are the primary erosion processes of all Be layer thicknesses (1 – 50 μm) on W surface at the plasma heat load of $0.2\ MJm^{-2}$. On W surface at $0.2\ MJm^{-2}$, all Be layer thicknesses tested retain their integrity up to the maximum pulse number, except at local defects and on tile edges.

At $0.5\ MJm^{-2}$ on W surface, Be layer melting, melt layer agglomeration and movement (probably driven by pressure forces) are the main damage processes, and occur immediately within a single pulse. Melting was observed not only the tile edges but also on the full tile surface. Melt layer movement lead to fully elimination Be layer near plasma facing edges even for maximum thickness of Be layer (55 μm) already after 2 pulses. But no significant melt splashing is observed, despite the far higher plasma pressure than expected in ITER. These results demonstrate that short transients of order of those specified for the maximum controlled ELM energy density required to avoid shallow surface melting of pure W surfaces in ITER will significantly erode, or completely remove Be layer co-deposits, but that significant dust generation may not occur. Since Be co-deposits are expected mostly in the divertor baffle areas, where ELM fluxes are lower, it is to be expected that disruptions, which may deposit high energy densities over a large target area, may be the principal cause of Be-layer damage or removal.

For Be layer deposited on the macrobrush bulk Be FW PFCs comparison between the different Be layer thicknesses after multiple plasma pulse exposure at heat loads of $0.2\ MJm^{-2}$ indicates different behavior for different thicknesses.

For 55 μm Be layer cracks formation and macroscopic flaking (the maximum size of the peels is 1 – 3 mm) are significantly intense as compare with lower thickness of Be layer and lead to catastrophic damages of Be layer already after 2 pulses. The cracks

formation and layer microscopic flaking (the maximum size of the peels is 10 – 50 μm) are the main damage processes of the target with 1 μm Be layer. These processes after 50 plasma pulses lead to significant Be layer losses in the range of 10 – 40%, which value is depend on location on the exposed surface.

The cracks formation was also observed on the target with 10 μm Be layer but this process was not lead to flaking and elimination of the 10 μm Be layer after 50 plasma pulses at 0.2 MJm^{-2} was not observed. For 10 μm Be layer changing of the Be layer microstructure due to melting and resolidification was observed mainly on the prominent area of the Be layer surface. The 10 μm Be layer retains its integrity after 50 plasma exposure at energy density of 0.2 MJm^{-2}.

Comparison between 10 μm and 55 μm Be layer thicknesses after multiple plasma pulse exposure at heat loads of 0.5 MJm^{-2} also indicates to higher resistance of 10 μm Be layer under plasma action.

The results of the performed experiments indicate to existence of optimal thickness of Be layer on the bulk Be surface (in the range of 1 – 55 μm), which is correspond to minimal erosion rate and maximum lifetime.

Acknowledgment

This work was supported by ITER Organization and Institution «Project Center ITER» (RF DA).

References

[1] R.A. Pitts, et al., J. Nucl. Mater. 415 (2011) S957–S964.
[2] R. Mitteau, et al., J. Nucl. Mater. 415 (2011) S969.
[3] K. Schmid, et al., Nucl. Fusion 55 (2015) 053015.
[4] A. Zhitlukhin, et al., J. Nucl. Mater. 363–365 (2007) 301.
[5] N. Klimov, et al., Phys. Scr. T145 (2011) 014064.
[6] G. Federici, et al., J. Nucl. Mater. 337–339 (2005) 684.
[7] N. Klimov, et al., J. Nucl. Mater. 390–391 (2009) 721.
[8] N. Klimov, et al., J. Nucl. Mater. 415 (2011) S59.
[9] N.S. Klimov, et al., J. Nucl. Mater. 438 (2013) S241–S245.
[10] D.V. Kovalenko, et al., Phys. Scr. T145 (2011) 014065.
[11] I.B. Kuprianov, et al., Phys. Scr. T145 (2011) 014063.
[12] N.S. Klimov, et al., Fusion Sci. Technol. 66 (#1) (2014) 118–124.
[13] C.P. Lungu, et al., Phys. Scr. T128 (2007) 157.
[14] T. Hirai, et al., Fusion Eng. Des. 83 (2008) 1072–1076.
[15] R. Raffray, G. Federici, J. Nucl. Mater. 244 (1997) 85–100.
[16] R. Raffray, G. Federici, J. Nucl. Mater. 244. (1997) 101–130.
[17] K. Schmidt, H. Hoven, K. Koizlik, J. Linke, H. Nickel, «Gefügeanalyse metallischer Werkstoffe – Interferenzschichten-Metallographie und Automatische Bildanalyse», Carl Hanser Verlag, München, 1985.